ELISA: A cryocooled 10 GHz oscillator with 10^{-15} frequency stability

S. Grop,[1] P. Y. Bourgeois,[1] N. Bazin,[1] Y. Kersalé,[1] E. Rubiola,[1] C. Langham,[2] M. Oxborrow,[2] D. Clapton,[3] S. Walker,[3] J. De Vicente,[4] and V. Giordano[1]
[1]*Department of Time and Frequency, FEMTO–ST Institute, UMR 6174 CNRS-ENSMM, 32 av. de l'Observatoire, Besançon Cedex 25044, France*
[2]*National Physical Laboratory, Queens Road, Teddington, Middlesex TW11 0LW, United Kingdom*
[3]*Oxford Instruments plc, Tubney Woods, Abingdon, Oxon OX13 5QX, United Kingdom*
[4]*European Space Agency ESA-ESOC, Robert Bosch Str. 5, Darmstadt D-64293, Germany*

(Received 18 September 2009; accepted 16 December 2009; published online 12 February 2010)

This article reports the design, the breadboarding, and the validation of an ultrastable cryogenic sapphire oscillator operated in an autonomous cryocooler. The objective of this project was to demonstrate the feasibility of a frequency stability of 3×10^{-15} between 1 and 1000 s for the European Space Agency deep space stations. This represents the lowest fractional frequency instability ever achieved with cryocoolers. The preliminary results presented in this paper validate the design we adopted for the sapphire resonator, the cold source, and the oscillator loop.
 [doi:10.1063/1.3290631]

I. INTRODUCTION

The ever increasing need for better tracking data and scientific return in deep space missions calls for the development of new frequency references of improved stability. The ground station of the European Space Agency (ESA) are currently equipped with hydrogen masers (HMs) which are the most stable commercial atomic clocks around 1000 s–1 day time scales. Cryogenic sapphire oscillators (CSOs) offer unbeatable stability performances in time scales ranging from milliseconds to a few hundred seconds, and therefore extremely low phase noise close to the carrier. A combined CSO and HM system in ESA deep space stations would allow to benefit from excellent short term and long stabilities. Compared to the current performance available from hydrogen masers and state-of-the-art quartz oscillators, CSO would provide the means to improve the orbit determination and would open the field to new radio science experiments. The objective of the project ELISA funded by ESA is the design, the breadboarding, and the validation of a CSO for ground station use, in line with a frequency stability specification of $\sigma_y(\tau)\leq 3\times10^{-15}$ for $1\ \mathrm{s}\leq\tau\leq1000$ s associated with a large autonomy, i.e., at least one year of continuous operation without maintenance.

Such a frequency performance has been already demonstrated by few laboratories operating whispering gallery mode sapphire resonators (WGMSRs) cooled into liquid helium Dewars.[1–4] A detailed review of the techniques used in the design and construction of these CSOs has been published recently.[5] Although this technology has already proved its ability to get the frequency stability specifications, it is not really suited for the ESA application which requires a large autonomy of the frequency reference. The objective of a continuous operation at least during one year rejects the use of a liquid helium Dewar which has to be refilled periodically. Some attempts have been realized few years ago by using single stage Gifford–McMahon cryocoolers.[6,7] Unfortunately, the lowest temperature provided by these cryocoolers did not permit to get entirely the benefit of the sapphire resonator which presents an optimal temperature around 6 K. Later Wang and Dick[8] experimented a compensated sapphire resonator at 10 K cooled into a two-stage Gifford-McMahon cryocooler which approached the ESA performances but still limited at 1×10^{-14} at 1 s and by a relatively large drift at long term, i.e., 1×10^{-13}/day. More recently, Watabe *et al.*[9] proposed the use of a two-stage pulse tube cryocooler which presents a higher durability and a lower level of vibrations than other types of cryocooler but the performances they obtained still remain limited above 1×10^{-14}.

This article presents the design, the breadboarding, and the validation of a CSO which we named "ELISA," built under contract of the ESA by the Femto-ST Institute (F) as the prime contractor, the National Physical Laboratory (U.K.) and the TimeTech company (D). In this CSO, the sapphire resonator is cooled into a closed cycle cryocooler specially designed to limit mechanical vibrations and thermal fluctuations. The autonomy of the whole system is thus the lifetime of the cryocooler (more than two years).

II. ELISA SUBSYSTEMS

The scheme in Fig. 1 describes the main subsystems constituting the ELISA frequency reference. The heart of the system is a WGMSR made of a large and thick high purity sapphire (HEMEX grade[10]) cylinder placed in the center of a copper cavity (see Sec. III). This assembly is thermally connected to the second stage of a pulse tube cryocooler. A special *soft* thermal link and a thermal ballast (see Sec. VI) were designed in order to filter the vibrations and the temperature modulation at about 1 Hz induced by the gas flow in the cryocooler.

Low thermal conductance coaxial cables are used to connect the sapphire resonator to the sustaining loop placed at room temperature. The oscillating circuit is completed by

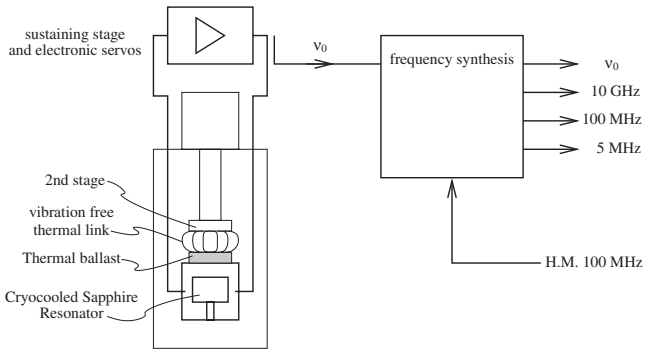

FIG. 1. ELISA subsystems. The frequency reference is a sapphire resonator maintained at a low temperature (≈ 6 K) into a closed cycle cryocooler. The CSO delivers a signal at the frequency ν_0 which serves as reference for a frequency synthesis subsystem delivering the useful frequencies.

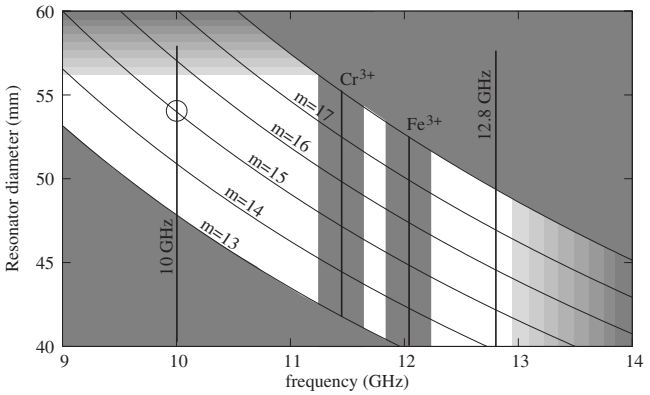

FIG. 2. Resonator frequency selection rules. The chosen resonator parameters correspond to the point highlighted by the circle: frequency $\nu_0 = 10$ GHz, diameter $D \approx 54$ mm, azimuthal number $m = 15$.

two servos stabilizing the phase along the loop and the power injected into the resonator. These control loops use the same principle than those described in the reference[5] (see Sec. V). Apart from the CSO signal at a frequency ν_0, we have to generate three other frequencies required for ESA applications: 10 GHz, 100 MHz, and 5 MHz. Moreover these useful signals should be phase locked at long term on a 100 MHz reference coming from a HM. A frequency synthesis was then designed to transfer the CSO's frequency stability to these useful signals with a slight degradation at 5 MHz as a result of the performance of typical rf components. In this paper, we will focus on the CSO only, the frequency synthesis, still not validated, will be detailed in a forthcoming paper.

III. SAPPHIRE RESONATOR

The frequency reference is a cylindrical sapphire resonator in which high order modes called whispering gallery (WG) modes can be excited. These modes are characterized by a high energy confinement in the dielectric due the total reflection at the vacuum-dielectric interface. As sapphire shows the lowest dielectric losses in the microwave range, a Q factor as high as 1×10^9 can be obtained at the liquid-He temperature. The useful modes are divided in two families: quasitransverse magnetic, designated as WGH, and quasitransverse electric (WGE) modes. They are further denoted by three integers: m, n and l. m is the number of wavelength in the azimuthal direction φ. n and l are the numbers of field nodes in the radial and axial direction, respectively. The modes of interest have generally $10 < m < 20$ and $n = l = 0$. In pure sapphire monocrystal, WG modes will have a monotonic frequency-versus-temperature law. The pure sapphire resonator do not have the frequency-versus-temperature turning point otherwise found in most piezoelectric resonators after appropriate design. Although the mode frequency thermal sensitivity decreases significantly at low temperature, it never goes low enough for the target stability to be achieved with state-of-the-art temperature control. Fortunately, it turns out that high-purity sapphire crystals always contain a small concentration of paramagnetic impurities, as Cr^{3+}, Fe^{3+} or Mo^{3+}. These ions induce a small magnetic permeability whose temperature dependence compensates for the natural sapphire resonator thermal sensitivity. It is then a result that the actual resonator frequency dependence on the temperature is quadratic. The resonator frequency reaches a maximal value at a specific temperature T_0. This turnover temperature T_0 depends on the mode and on the impurity concentration but for many of the resonators tested by different groups, the turnover temperature is generally in the range of 5–8 K. This thermal compensation relaxes dramatically the thermal stabilization requirements. Indeed, around T_0 the residual quadratic thermal sensitivity of the resonator frequency $(1/\nu) \times (d^2\nu/dT^2)$ is of the order of few 10^{-9} K^{-2}.[11] With such a thermal compensation phenomena, the frequency stability objective of 3×10^{-15} can be obtained with a ± 1 mK thermal stabilization which can be easily fulfilled with commercial cryogenic temperature controllers.

The resonator size and WG mode order determine the resonant frequency and the unloaded Q factor. Experience shows that the best results are obtained with a resonator presenting a ratio diameter over height of the order of $D/H \approx 3/5$ (Ref. 12) and with WG modes between 13 and 18. The energy confinement in the dielectric improves as the mode order increases. This fact has two practical consequences: (1) Q is progressively degraded at lower-order modes (less than 13) because of electromagnetic radiation, and (2) high order modes (greater than 18) are difficult or impossible to exploit because the couplers need too sharp adjustment. Another difficulty connected with high-order modes is the presence of many spurious modes, which makes the frequency selection difficult. For practical reasons the resonator size cannot be too large. A resonator diameter D of about 50 mm is comfortable for mechanics and cryogenics. This means that the resonant frequency should not be lower than some 9 GHz. Dielectric dissipation in sapphire increases as frequency increases. This phenomenon sets a soft upper limit at some 13 GHz. This limit is about independent of the resonator size. Finally, the resonance of the Cr^{3+} ion at 11.45 GHz, and the resonance of the Fe^{3+} ion and 12.04 GHz are to be avoided. A margin of ± 200 MHz is recommended. Figure 2 summarizes the frequency selection rules we adopted. This figure represents the relation between the resonator diameter and its resonance frequency for the WGH mode family assuming $D/H = 3/5$.

A. Design strategy

It is generally agreed that the resonator is the core of the oscillator, which determines the frequency stability. Provided the criteria discussed at the beginning of Sec. III are met, the most critical parameters are the quality factor Q and the thermal stability of the natural frequency in the vicinity of the turnover temperature. As a consequence, the physicist is inclined to start from a set of available resonators, identify the highest-Q mode, check on the thermal stability, and build the entire oscillator around this empirical choice. One problem with this approach is that the frequency synthesizer, needed for the oscillator to deliver a suitable round frequency, has to provide an interpolation frequency in a wide range, up to 1 GHz. Implementing such synthesizer with microhertz resolution, and with stability and spectral purity high enough not to degrade the output signal, is not simple. Another problem is that each resonator has its own optimal frequency, which determines the design of the electronics. This turns into a technical difficulty if more than one oscillator will be needed in the future, or if the resonator has to be replaced for any reason.

Aware of all these problems, we opted for a different approach based on the criteria discussed underneath. After refining the electromagnetic model,[13] we are able to design a resonator with a high-Q mode at the frequency ν_0 of our choice. The electrical and mechanical tolerances yield a frequency accuracy of 5×10^{-4} (±5 MHz at 10 GHz) and a reproducibility of 10^{-4} (±1 MHz at 10 GHz). That said, we chose a resonant frequency $\nu_0=\nu_{00}-\delta_{\mathrm{rf}}$, where ν_{00} is a comfortable round value, and $\delta_{\mathrm{rf}}=10\pm5$ MHz. This choice is justified by the fact that a single-chip direct digital synthesizer (DDS) has the desired resolution and provides sufficient stability and spectral purity if the output frequency does not exceed some 15–20 MHz. Additionally, δ_{rf} cannot be too low frequency (<5 MHz), otherwise it is difficult to avoid the spur of frequency ν_0, too close to ν_{00}. In this conditions, a DDS fits the needs for the correction δ_{rf} The nominal size of the resonator makes $\nu_0<\nu_{00}$, so the correction $-\delta_{\mathrm{rf}}$ takes a negative value. It is still possible to thin the resonator so that $\nu_0=\nu_{00}+\delta_{\mathrm{rf}}$, which can fix a number of mistakes without modifying the electronics.

Figure 2 suggests that ν_{00} can be either 10 or 12.8 GHz, so that a low-noise 100 MHz output can be obtained from a cascade of by 10 or power-of-two frequency dividers. The value $\nu_{00}=10$ GHz has been chosen because low-flicker SiGe amplifiers[14,15] are available at this frequency, while 12.8 GHz falls beyond a sharp cutoff.

Our design strategy has three additional merits connected to the low value of the interpolation frequency δ_{rf}. The first one is that it simplifies the synthesizer. The second one is that the synthesizer can be overengineered for high stability and low noise at a reasonably low cost. If a lucky oscillator exceeds the expected stability, the benefit is not lost. The third one is that the synthesizer can be tested without the oscillator, which simplifies the logistics and speeds up the validation process.

FIG. 3. (Color online) The two HEMEX grade sapphire resonators.

B. Resonator realization and validation

The key parameters to accurately determine the modes frequencies are the values of the sapphire tensor permittivity components used for the calculation. By comparing experimental frequencies of available crystals and simulation results, we deduced the values of the permittivity components at 4 K to be: $\varepsilon_{\perp}=9.270\,688$ and $\varepsilon_{\parallel}=11.340\,286$. Eventually, by using a finite elements analysis, we get a $\mathrm{WGH}_{15,0,0}$ mode at 9.99 GHz with $D=54.2$ mm and $H=30$ mm. Taking into account the machining possibilities and the cost, we eventually ordered two sapphire pieces with $D=54.2\ \mathrm{mm}\pm10\ \mu\mathrm{m}$ and $H=30\ \mathrm{mm}\pm20\ \mu\mathrm{m}$. The resonator frequency is then defined as $9.99\ \mathrm{GHz}\pm3.5\ \mathrm{MHz}$.

The resonator has a spindle (diameter 10 mm, length 22 mm) to be clamped from below. Such a mounting enables to reduce the mechanical stress on the region where the electromagnetic field is confined.[16] Two quasi-identical resonators were machined from the same HEMEX sapphire boule by the Crystal System company. These two resonators named ELISA and ALIZÉE are shown on the Fig. 3. The cryogenic microwave resonator making up the ELISA's frequency reference is represented in the Fig. 4.

The resonator is clamped on the inferior plate closing the gold-plated copper cavity. The latter is maintained in thermal contact with the cooling source through a copper piece in which a thermal sensor and a heater are anchored. To couple the resonator to the external circuit, we use two small magnetic loops intercepting the H_{φ} magnetic field component of

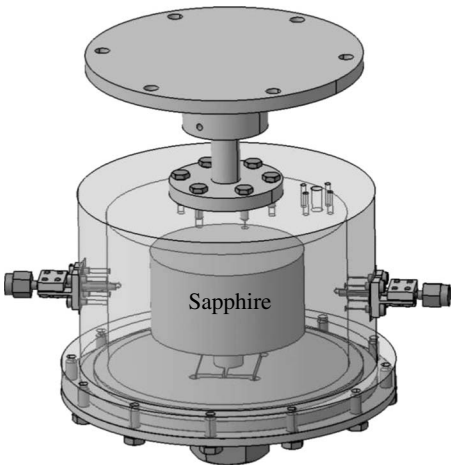

FIG. 4. ELISA resonator design.

TABLE I. Resonators parameters.

	ν_0 (GHz)	T_0 (K)	Q_L	β_1	β_2	IL (dB)
ELISA	9.989 121	6.12	7.4×10^8	1	≈0.02	−24.9
ALIZÉE	9.988 370	6.05	6.9×10^8	1.09	≈0.02	−26

the resonator. By varying the penetration depth of the loop into the cavity, we can adjust the input (β_1) and output (β_2) coupling coefficients. To maximize the sensitivity of the frequency discriminator used to control the phase along the oscillating loop, β_1 has to be set near the unity. On the contrary β_2 has to be set to a low value to not degrade the loaded Q factor, but sufficiently high to limit the resonator insertion losses (IL). Table I summarizes the main characteristics of the two resonators at their turnover temperature T_0. The adjustment of the coupling coefficients has been obtained after few cooldowns.

Figure 5 shows the modulus of the ELISA transmission coefficient around the $WGH_{15,0,0}$ mode frequency in a 1 kHz span. The resonator bandwidth is 14 Hz. Figure 6 represents the variation in the ELISA's $WGH_{15,0,0}$ mode frequency as a function of the resonator temperature. These experimental data have been fitted with a second order polynomial to get the turnover temperature T_0.

IV. CRYOCOOLER

To achieve the required oscillator frequency stability, the oscillator's sapphire resonator must be maintained in a cryogenic environment that is sufficiently free of mechanical vibration and where the resonator's temperature is uniform and precisely controlled at a specific value. Two options were available at the beginning of the ELISA project: using a liquid helium cryostat or a cryogen-free cryocooler-based cryostat.

With a bath cryostat, the vacuum can in which the resonator resides is surrounded by a bath of cryogenic liquid (in this case liquid helium); within a Dewar. Such an arrangement naturally provides the sapphire resonator with a thermally uniform environment, relatively free of mechanical vibration (except from bubbling). Cryostats based on cryocoolers, on the other hand, will generally subject the resonator to unacceptable levels of mechanical vibration and thermal nonuniformity (i.e., temperature gradients) unless the cryostat is designed in such a way that these perturbations are suppressed.

The key point that made us opt for the cryocooler option is that unlike bath cryostat, they do not need regular refills of liquid helium. These refillings disturb the sapphire resonator which needs around two days to recover. Nevertheless two problems had to be solved: the vibrations level and the temperature fluctuations of the cryocooler cold stage. The resonator fractional frequency sensitivity to a constant vertical acceleration has been estimated to be $-3.2\times10^{-10}/g$ (Ref. 17) and we measured temperature fluctuations of ±100 mK on a Cryomech PT405 with a 1.3 Hz frequency corresponding to the gas cycle in the system.

Oxford Instruments supplied a 4K Cryofree® cryostat modified to achieve the performances required by the ELISA project. Those were a low displacement on the experiment plate (less than 2 μm in three axes) with a temperature stabilization of ±1 mK over 1000 s and a cooling power at 4 K of 50 mW. The cryocooler used by Oxford Instruments is a two-stage pulse-tube refrigerator with a rotary valve decoupled from the main Dewar, eliminating the need for moving parts in the cold head. The cryostat design of the vibration reduction system is similar to those described in the references.[18,19] The Oxford Instruments design is represented in Fig. 7.

The two stages of the cryostat (77 K shield and 4 K cold plate) are thermally linked to the cryocooler stages with floppy copper heat links. The support thin-wall tubes are mounted like a hexapod to give rigidity to the system. To limit the temperature fluctuations of the cold stage, a gadolinium gallium garnet crystal[20] was mounted between this

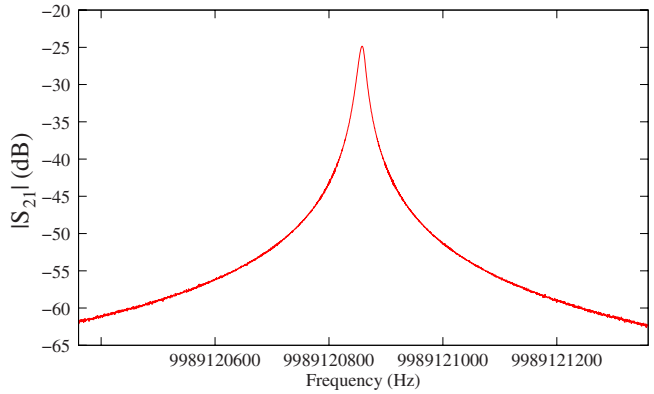

FIG. 5. (Color online) ELISA transmission coefficient around the $WGH_{15,0,0}$ mode frequency. Frequency span 1 kHz.

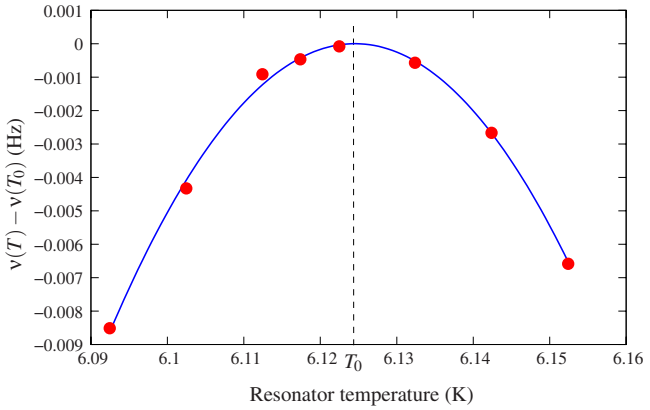

FIG. 6. (Color online) Resonator frequency vs temperature around the turnover temperature T_0=6.12 K.

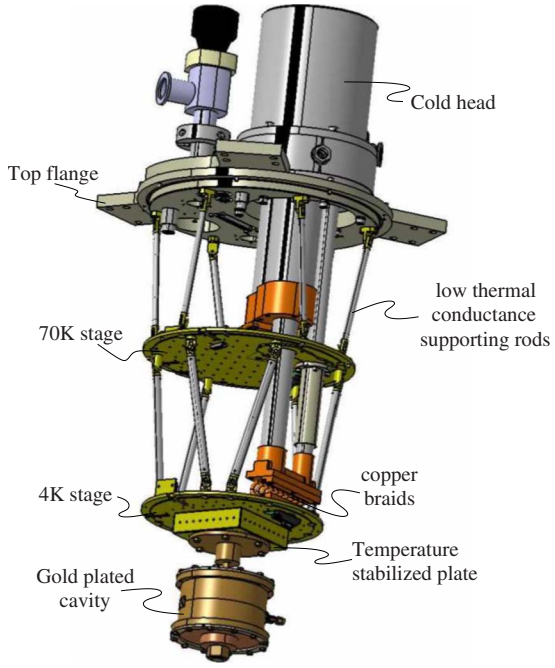

FIG. 7. (Color online) Crycooler internal design.

stage and a copper temperature stabilization block supporting the experiment using four legs. The four legs provided a tuned weak thermal link to again optimize the temperature stability and cooling power of the cryostat. Few combinations of materials for the legs were used and the optimized performance was obtained when using two stainless steel and two brass/copper legs. To check the temperature stability on the experimental plate, we fixed on it an independent high resolution thermal sensor and recorded the measured temperature. Calculating the Allan deviation of the recorded samples we get the temperature versus integration time stability showed in Fig. 8. Although we observed a bump on the temperature stability curve around an integration time of about 20 s, the temperature stability requirement, i.e., $\Delta T \leq 1$ mK rms, is totally fulfilled.

A three-axis accelerometer was fixed on the experimental plate and we measured less than 1 μm vibration in x, y, and z directions.[21] The base temperature at stabilization stage with the customer wiring is 6 K with 50 mW applied to the stabilization stage.

V. OSCILLATOR

The oscillator circuit is described in Fig. 9. It is a classical transmission oscillator circuit with two additional servo loops that control the phase and the power of the circulating signal. These two servos are mandatory to get a high frequency stability.

Without these two servo loops, the CSO frequency stability will stay limited to some 1×10^{-13} at short term and will be furthermore degraded at long integration time due to the environmental sensitivity of the circuit. The first servo loop is based on the Pound frequency discriminator principle,[22–24] it ensures that the CSO oscillates at the resonator frequency ν_0 by compensating any variation in the phase lag along the loop. It uses a phase modulation at a

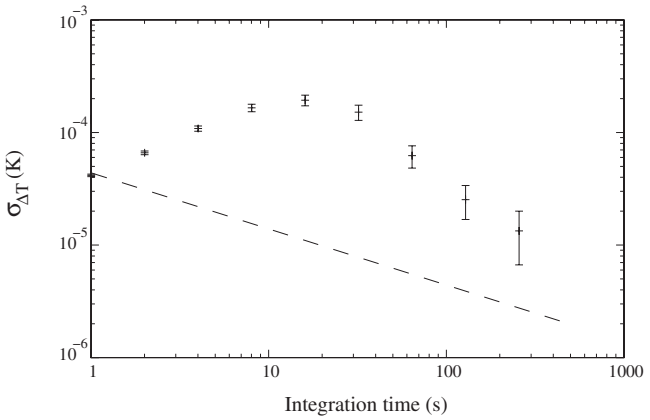

FIG. 8. Measured temperature stability on the experimental plate. The dashed line represents the temperature measurement resolution.

frequency of the order of few tens of kHz to probe the resonance. The phase modulation is applied to the microwave signal through a first voltage controlled phase shifter (VCPS 1). A lock-in amplifier demodulates the signal reflected by the resonator to generate an error signal which is eventually added to the dc bias of a second voltage controlled phase shifter (VCPS 2). Due to the radiation pressure and to the self-resonator heating, the resonator frequency presents a power sensitivity of the order of 4×10^{-11}/mW. The power servo loop ensures that the power injected into the resonator stays constant. A tunnel diode placed as near as possible to the resonator input enables to get a voltage proportional to the signal power. This voltage is compared to a high stability voltage reference and the resulting error signal is used to control the bias of a voltage controlled attenuator. As explained in Ref. 5 the modulating signal applied to VCPS 1 induces as well an undesirable amplitude modulation (AM) which shifts the oscillating frequency from ν_0. As the frequency shift is dependant on the AM index, the CSO frequency stability will be limited by the variations in the VCPS ILs which in turn couples the CSO frequency to environment and especially to the room temperature. A solution has been proposed to surpass this last limitation,[5,25] but at this stage of development we did not yet implement such a supplementary control on our CSO. The result we obtain demonstrates that this effect did not affect the CSO frequency stability above 3×10^{-15}.

VI. FREQUENCY PERFORMANCES

To evaluate the relative frequency stability of the cryocooled CSO ELISA, it has been compared with a second CSO built around the second resonator ALIZÉE which is cooled in a liquid helium Dewar. Apart from the cooling method, the two CSOs are quasi-identical.

Before running ELISA into the cryocooler, some preliminary measurements have been realized with the two resonators cooled in liquid helium Dewar.[21] The results obtained few months ago have demonstrated that the liquid helium-cooled CSO presents a short term relative frequency instability less or equal to 3×10^{-15}. After this first attempt that has proved the quality of the oscillator design, we integrated one resonator into the cryocooler. A new determination of the

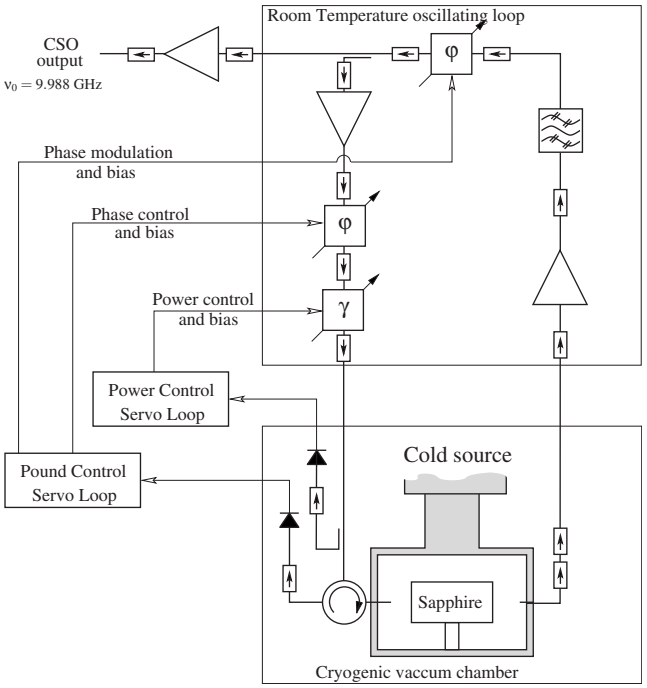

FIG. 9. ELISA oscillator design. The sustaining loop is completed with two additional servo loops stabilizing the phase of the circulating signal and the power injected inside the resonator.

relative frequency stability has been performed. Any degradation in the ELISA's frequency stability due to some residual mechanical vibrations into the cryocooler should then be detected. The measurement technique is a standard one: the two oscillator signals are mixed to get a beatnote at the frequency difference which is of about 750 kHz. The beat signal is directly send to a high resolution counter and the Allan deviation σ_y is computed from data averaged over 1 s. Figure 10 shows σ_y as a function of the integration time τ. The 3×10^{-15} frequency stability specification is almost met for $\tau \leq 1000$ s. This result corresponds to a data recording of about 7 h without any postprocessing applied to the raw data.

A rapid view on this Allan deviation curve shows that the measured frequency stability appears limited at short term by a "plateau" just below 3×10^{-15}. We are confident that the observed plateau does not correspond to a flicker frequency noise but more certainly to the superposition of

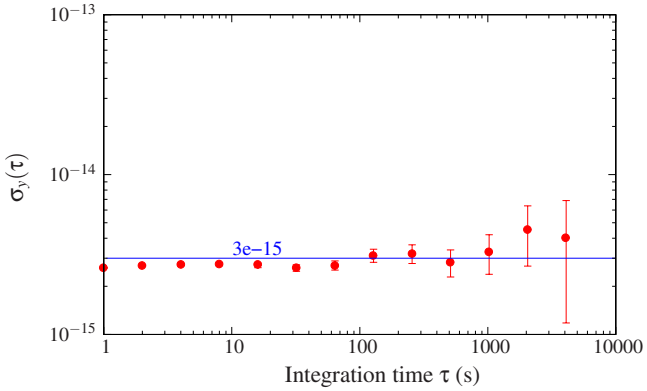

FIG. 10. (Color online) Maximal frequency instability of the cryocooled CSO ELISA measured by direct comparison with a liquid helium-cooled sapphire oscillator.

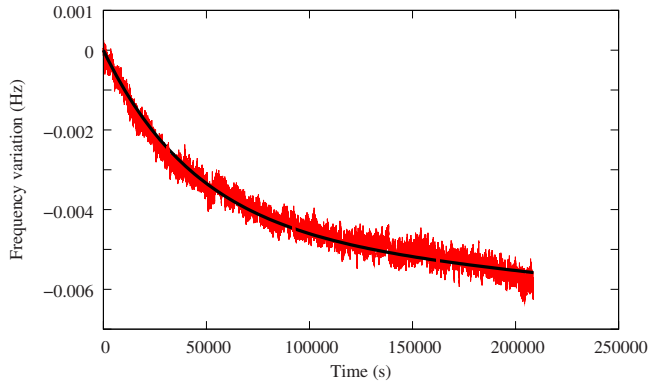

FIG. 11. (Color online) Evolution of the beatnote frequency after refilling.

some residual frequency deterministic variations. We detected recently that the thermostat stabilizing the voltage references used both for power and frequency servo suffer from a small but detectable pumping at a rate of the order of 300 s. Power servos which are more sensible to the voltage reference noise have been modified but the same issue still subsists in the Pound loops. That can explain the little bumps in the σ_y curve around 300 s.

When two almost equivalent oscillators are directly compared, it is a common practice to divide the measured Allan deviation by $\sqrt{2}$ assuming the two oscillator noises are equivalent and uncorrelated. We did not apply this rule in our case because, although build with practically identical resonators, the two CSOs behave differently. All the parameters related to the servo loops as the integrator outputs and the lock-in output noise are much more stable for the cryocooled CSO. In the case of the liquid helium Dewar CSO, the sustaining loop has a length of about 4 m. The cables linking the resonator to the sustaining circuit pass through the helium bath. Due to the helium evaporation their electrical length and loss are continuously varying. Moreover, the almost critical input coupling that we fortunately get for ELISA should limit the effect of AM-index fluctuations.[5] Eventually the liquid helium Dewar has to be refilled every week. This operation pertubes the CSO frequency which takes time to stabilize. As helium evaporates continuously we doubt that the liquid helium CSO get its equilibrium between two refillings. Figure 11 shows the beatnote frequency variations after refilling.

We note that more than one day is needed to get the best estimation of the frequency stability. Nevertheless, after 200 000 s the residual frequency drift is less than 5×10^{-14}/day. Eventually although there are obviously still some margins to improve the result, we demonstrate in this paper that the cryocooled CSO can meet the frequency stability specification of 3×10^{-15} up to 1000 s integration times.

[1] S. Chang, A. G. Mann, and A. N. Luiten, Electron. Lett. **36**, 480 (2000).
[2] G. Marra, D. Henderson, and M. Oxborrow, Meas. Sci. Technol. **18**, 1224 (2007).
[3] K. Watabe, J. Hartnett, C. R. Locke, G. Santarelli, S. Yanagimachi, T. Ikegami, and S. Ohshima, Proceedings of the 20th European Frequency and Time Forum, Braunschweig, Germany, 27–30 March 2006, pp. 92–95.
[4] P. Y. Bourgeois, F. Ladret-Vieudrin, Y. Kersalé, N. Bazin, M. Chaubet, and V. Giordano, Electron. Lett. **40**, 605 (2004).

[5] C. R. Locke, E. N. Ivanov, J. G. Hartnett, P. L. Stanwix, and M. E. Tobar, Rev. Sci. Instrum., **79**, 051301 (2008).
[6] L. Hao, N. Klein, J. C. Gallop, W. J. Radcliffe, and I. S. Ghosh, IEEE Trans. Instrum. Meas. **48**, 524 (1999).
[7] Y. Kersalé, S. Vives, C. Meunier, and V. Giordano, IEEE Trans. Ultrason. Ferroelectr. Freq. Control **50**, 1662 (2003).
[8] R. T. Wang and G. J. Dick, IEEE Trans. Instrum. Meas. **48**, 528 (1999).
[9] K. Watabe, Y. Koga, S. Ohshima, T. Ikegami, and J. Hartnett, *Proceedings of the 2003 IEEE International Frequency Control Symposium*, Tampa, FL, 4–8 May 2003 (IEEE, New York, 1992).
[10] For more information about the high quality sapphire crystal, see www.crystalsystems.com/
[11] A. N. Luiten, A. G. Mann, M. E. Costa, and D. G. Blair, IEEE Trans. Instrum. Meas. **44**, 132 (1995).
[12] J. Krupka, D. Cros, A. Luiten, and M. Tobar, Electron. Lett. **32**, 670 (1996).
[13] S. Grop, V. Giordano, P. Bourgeois, Y. Kersalé, N. Bazin, M. Oxborrow, G. Marra, C. Langham, E. Rubiola, and J. De Vicente, *Proceedings of the Microwave Technology and Techniques Workshop 2008-Innovations and Challenges*, 6–7 May 2008 (ESA/ESTEC, Noordwijk, 2008).
[14] For more information about the low noise SiGe microwave amplifiers, see www.amlj.com/lowphasenoise.html/
[15] E. Rubiola, *Phase Noise and Frequency Stability in Oscillators* (Cambridge University Press, Cambridge, 2008).
[16] S. Chang and A. Mann, Proceedings of the 2001 IEEE International Frequency Control Symposium, Seattle, WA, 6–8 June 2001, pp. 710–714.
[17] M. Oxborrow, K. Benmessaï, S. Grop, N. Bazin, P. Y. Bourgeois, Y. Kersalé, and V. Giordano, Proceedings of the European Frequency and Time Forum (EFTF08), Toulouse, France, 23–25 April 2008.
[18] T. Tomaru, T. Suzuki, T. Haruyama, T. Shintomi, N. Sato, A. Yamamoto, Y. Ikushima, R. Li, T. Akutsu, T. Uchiyama, and S. Miyoki, *Cryocoolers 13* (Springer, New York, 2005).
[19] S. Caparrelli, E. Majorana, V. Moscatelli, E. Pascucci, M. Perciballi, P. Puppo, P. Rapagnani, and F. Ricci, Rev. Sci. Instrum. **77**, 095102 (2006).
[20] W. Dai, E. Gmelin, and R. Kremer, J. Phys. D: Appl. Phys. **21**, 628 (1988).
[21] S. Grop, V. Giordano, P. Y. Bourgeois, N. Bazin, Y. Kersalé, M. Oxborrow, G. Marra, C. Langham, E. Rubiola, and J. de Vicente , Proceedings of the Joint Meeting IFCS-EFTF, Besançon, France, 20–24 April 2009, pp. 376–380.
[22] R. Drever, J. Hall, F. Kowalski, J. Hough, G. Ford, A. Munley, and H. Ward, Appl. Phys. B: Lasers Opt. **31**, 97 (1983).
[23] Z. Galani, W. M. Bianchini, Jr., C. Raymond, R. Dibiase, R. Laton, and J. B. Cole, IEEE Trans. Microwave Theory Tech. **32**, 1556 (1984).
[24] E. Black, Am. J. Phys. **69**, 79 (2001).
[25] A. Luiten, "Sapphire Secondary Srequency Standards," Ph.D. thesis, University of Western Australia, 1995.